

Gravitational wave background in perfect fluid quantum cosmologies

Patrick Peter*

*GReCO – Institut d’Astrophysique de Paris, UMR7095 CNRS,
Université Pierre & Marie Curie, 98 bis boulevard Arago, 75014 Paris, France*

Emanuel J. C. Pinho[†] and Nelson Pinto-Neto[‡]

*Lafex - Centro Brasileiro de Pesquisas Físicas – CBPF,
rua Xavier Sigaud, 150, Urca, CEP22290-180, Rio de Janeiro, Brazil*

(Dated: June 30, 2018)

We discuss the gravitational wave background produced by bouncing models based on a full quantum evolution of a universe filled with a perfect fluid. Using an ontological interpretation for the background wave function allows us to solve the mode equations for the tensorial perturbations, and we find the spectral index as a function of the fluid equation of state.

PACS numbers:

I. INTRODUCTION

The theory of cosmological perturbations [1] relies essentially on two assumptions, namely that the background is described by pure classical General Relativity (GR), while the perturbations thereof stem from quantum fluctuations, although they are subsequently evolved classically. Quite apart from the computational usefulness of this scheme, this state of affairs is rather incomplete, and one would expect instead a fully quantum treatment of both the background and the perturbations to be achievable. In fact, the overwhelming majority of classical backgrounds possess an initial singularity at which the classical theory is expected to break down. In recent years, many quantum background cosmological models have been proposed, which share the attractive property of exhibiting neither singularities nor horizons [2, 3, 4], leading the universe evolution through a bouncing phase due to quantum effects, and a contracting phase from infinity before the bounce. These new features of the background introduce a new picture for the evolution of cosmological perturbations: vacuum initial conditions may now be imposed when the Universe was very big and almost flat, and effects due to the contracting and bouncing phases, which are not present in the standard background model, may change the subsequent evolution of perturbations in the expanding phase. Hence, it is quite important to study the evolution of perturbations in these quantum backgrounds. The aim of the present paper is to provide a step in this direction by considering tensor perturbations in quantum minisuperspace background solutions. Interpreting the quantum theory in an ontological way [5, 6] allows to define quantum scale factor trajectories, which can then be used in the second order tensorial modes perturbation equations

as show in Ref. [7].

Note that such models may be viewed as alternatives to the standard inflationary paradigm [8]. Most known alternatives [9, 10] to inflation present a primordial bouncing phase [11, 12]. Note that such a phase can also be seen as a complementary ingredient necessary for a complete cosmological scenario to make actual sense, *i.e.* not to be plagued with a singularity [13], or to avoid facing any trans-Planckian problem [14] if, for instance, the bounce occurs at a scale such that all relevant cosmological scales now never went trans-Planckian. The bounce phase has recently been the subject of a lot of attention, in particular in view of the fact that in many instances, it was found to have the ability to modify the primordial spectrum of scalar perturbations, thus paving the way to confront them to the observational data [15]. In the case of bounces in quantum cosmological models, although the evolution equations for the perturbations may be constructed [16], they are rather complicated due to the fact that the background does not satisfy classical Einstein’s equations. Hence, all works in this area had to rely on a semiclassical approximation.

In this paper, we calculate the gravitational wave background spectrum produced at the bounce transition when this phase is described by a perfect fluid and the theory is fully quantized: this is the first time such a calculation, not involving any semiclassical approximation is performed. The restriction to gravitational waves stems from the fact that the perturbation equations for this type of modes can be substantially simplified, even when the background is quantized [7]. Scalar and vector modes, however, exhibit technical difficulties which have not been solved yet, so that tensor modes are, for the time being, the only modes that can be studied in a completely quantum way.

The paper is organized as follows. Recalling in Sec. II how the ontological interpretation allows a simple separation between the background and the perturbations, we explain in Sec. III how the Bohmian trajectories for the scale factor are derived, and discuss their generality. Then, Sec. IV, which is the core of this work, provides

*Electronic address: peter@iap.fr

[†]Electronic address: emmanuel@cbpf.br

[‡]Electronic address: nelsonpn@cbpf.br

the tensorial modes indices in the known cases. We end in Sec. V with conclusions and discussions.

II. THE MODE EQUATION

The action we shall begin with is that of GR with a perfect fluid, the latter being described by the formalism due to Schutz [17], *i.e.*

$$\mathcal{S} = \mathcal{S}_{\text{GR}} + \mathcal{S}_{\text{fluid}} = -\frac{1}{6\ell_{\text{Pl}}^2} \int \sqrt{-g} R d^4x + \int \sqrt{-g} p d^4x, \quad (1)$$

where $\ell_{\text{Pl}} = (8\pi G_{\text{N}}/3)^{1/2}$ is the Planck length in natural units ($\hbar = c = 1$), p is the perfect fluid pressure whose density ρ is provided by the relation $p = \omega\rho$, ω being

a constant. The metric \mathbf{g} in Eq. (1) is of the Friedman-Lemaître-Robertson-Walker (FLRW) type, whose line element we choose to be given by

$$ds^2 = N^2(\tau) d\tau^2 - a_{\text{phys}}^2(\tau) (\gamma_{ij} + w_{ij}) dx^i dx^j, \quad (2)$$

i.e. we assume it is perturbed to first order and restrict attention to tensorial perturbations only, with $w^{\bar{i}\bar{j}}|_{\bar{j}} = 0$ and $w^{\bar{i}}_{\bar{i}} = 0$, indices being raised and lowered by means of the background metric γ_{ij} of the spacelike hypersurfaces (the bar denotes a covariant derivative with respect to this metric); the lapse function $N(\tau)$, once fixed, defines the gauge.

After inserting Eq. (2) into the action (1), and performing Legendre and canonical transformations, the Hamiltonian up to second order reads (see Ref. [7] for details)

$$\begin{aligned} H &\equiv NH_0 \\ &= N \left\{ -\frac{P_a^2}{4a} - \mathcal{K}a + \frac{P_\tau}{a^{3\omega}} \left(1 + \frac{\omega}{4} \int d^3x \gamma^{1/2} w_{ij} w^{ij} \right) + \frac{5P_a^2}{48a} \int d^3x \gamma^{1/2} w_{ij} w^{ij} \right. \\ &\quad \left. + \int d^3x \left[\frac{6\Pi_{ij}\Pi^{ij}}{a^3\gamma^{1/2}} + 2\frac{P_a w_{ij}\Pi^{ij}}{a^2} + \gamma^{1/2} a \left(\frac{w^{ij|k} w_{ij|k}}{24} + \frac{\mathcal{K}}{6} w_{ij} w^{ij} \right) \right] \right\}, \end{aligned} \quad (3)$$

which is nothing but the Hamiltonian of Ref. [16] expressed for a perfect fluid. In Eq. (3) and in what follows, we shall denote by \mathcal{K} the spatial curvature ($\mathcal{K} = 0, \pm 1$ for flat, open and closed space respectively) in order to avoid confusion with the wavenumber k below. The quantities P_a, Π^{ij}, P_τ are the momenta canonically conjugate to the scale factor, the tensor perturbations, and to the fluid degree of freedom, respectively. These quantities have been redefined in order to be dimensionless. For instance, the physical scale factor a_{phys} can be obtained from the adimensional a present in (3) through $a_{\text{phys}} = \ell_{\text{Pl}} a / \sqrt{V}$, where V is the comoving volume of the background spacelike hypersurfaces. This Hamiltonian, which is zero due to the constraint $H_0 \approx 0$, yields the correct Einstein equations both at zeroth and first order in the perturbations, as can be checked explicitly. In order to obtain its expression, no assumption has been made about the background dynamics.

In the quantum regime, this Hamiltonian can be substantially simplified through the implementation of the quantum canonical transformation generated by

$$U = \exp(iG_q) \equiv \exp\left(\frac{i}{12}\hat{\beta}_a\hat{Q}\right), \quad (4)$$

where $\hat{\beta}_a \equiv \frac{1}{2}(\hat{P}_a\hat{a} + \hat{a}\hat{P}_a)$ and $\hat{Q} \equiv \int d^3x \gamma^{1/2} \hat{w}_{ij} \hat{w}^{ij}$ are the self-adjoint operators associated with the corresponding classical variables, yielding, for a particular factor ordering of (3) (see Ref. [7] for details),

$$\hat{H}_0 = \left[-\frac{1}{4\hat{a}} \hat{P}_a^2 - \mathcal{K}\hat{a} + \frac{\hat{P}_\tau}{\hat{a}^{3\omega}} + \int d^3x \left(6\frac{\hat{\Pi}^{ij}\hat{\Pi}_{ij}}{\gamma^{1/2}a^3} + \frac{1}{24}\gamma^{1/2}a\hat{w}_{ij|k}\hat{w}^{ij|k} + \frac{1}{12}\gamma^{1/2}\mathcal{K}\hat{w}_{ij}\hat{w}^{ij} \right) \right]. \quad (5)$$

As we are here also quantizing the background, the quantization procedure is now to impose $\hat{H}_0\Psi(a, w_{ij}) = 0$. The Wheeler-DeWitt equation in this case reads

$$\begin{aligned} i\frac{\partial\Psi}{\partial T} &= \hat{H}_{\text{red}}\Psi \\ &:= \left\{ \frac{a^{3\omega-1}}{4} \frac{\partial^2}{\partial a^2} - \mathcal{K}a^{3\omega+1} + \int d^3x \left[-6\frac{a^{3(\omega-1)}}{\gamma^{1/2}} \frac{\delta^2}{\delta w_{ij} \delta w^{ij}} + a^{3\omega+1} \left(\gamma^{1/2} \frac{w_{ij|k} w^{ij|k}}{24} + \mathcal{K} \frac{w_{ij} w^{ij}}{12} \right) \right] \right\} \Psi, \end{aligned} \quad (6)$$

where we have chosen T as the time variable, which is equivalent to impose the time gauge $N = a^{3\omega}$. Note that such a choice is possible in the case at hand because we are considering a perfect fluid, for which one can use the variable which describes the fluid as a clock [18, 19].

Now, if one uses an ontological interpretation of quantum mechanics like the one suggested by de Broglie and Bohm [5], and makes the separation ansatz for the wave functional $\Psi[a, w_{ij}, T] = \varphi(a, T)\psi[a, w_{ij}, T]$, with $\psi[a, w_{ij}, T] = \psi_1[w_{ij}, T] \int da \varphi^{-2}(a, T) + \psi_2[w_{ij}, T]$, then Eq. (6) can be split into two, yielding

$$i \frac{\partial \varphi}{\partial T} = \frac{a^{3\omega-1}}{4} \frac{\partial^2 \varphi}{\partial a^2} - \mathcal{K} a^{3\omega+1} \varphi, \quad (7)$$

and

$$i \frac{\partial \psi}{\partial T} = \int d^3x \left[-6 \frac{a^{3(\omega-1)}}{\gamma^{1/2}} \frac{\delta^2}{\delta w_{ij} \delta w^{ij}} + a^{3\omega+1} \left(\gamma^{1/2} \frac{w_{ij|k} w^{ij|k}}{24} + \mathcal{K} \frac{w_{ij} w^{ij}}{12} \right) \right] \psi. \quad (8)$$

Using the Bohm interpretation, Eq. (7) can now be solved as in Ref. [2, 3, 4], yielding a Bohmian quantum trajectory $a(T)$, which in turn can be used in Eq. (8). Indeed, since one can view $a(T)$ as a function of T , it is possible to implement the canonical transformation generated by

$$U = \exp \left[i \left(\int d^3x \gamma^{1/2} \frac{\dot{a} w_{ij} w^{ij}}{2a} \right) \right] \exp \left\{ i \left[\int d^3x \left(\frac{w_{ij} \Pi^{ij} + \Pi^{ij} w_{ij}}{2} \right) \ln \left(\frac{\sqrt{12}}{a} \right) \right] \right\}, \quad (9)$$

where, as $a(T)$ is a given quantum trajectory coming from Eq. (7), Eq. (9) must be viewed as the generator of a time dependent canonical transformation to Eq. (8). It yields

$$i \frac{\partial \psi}{\partial T} = \int d^3x \left[-\frac{a^{3\omega-1}}{2\gamma^{1/2}} \frac{\delta^2}{\delta \mu_{ij} \delta \mu^{ij}} + a^{3\omega-1} \left(\gamma^{1/2} \frac{\mu_{ij|k} \mu^{ij|k}}{2} + \mathcal{K} \mu_{ij} \mu^{ij} - \frac{\ddot{a}}{2a} \mu_{ij} \mu^{ij} \right) \right] \psi. \quad (10)$$

Through the redefinition of time $a^{3\omega-1} dT = d\eta$, we obtain

$$i \frac{\partial \psi(\mu_{ij}, \eta)}{\partial \eta} = \int d^3x \left\{ -\frac{1}{2\gamma^{1/2}} \frac{\delta^2}{\delta \mu_{ij} \delta \mu^{ij}} + \gamma^{1/2} \left[\frac{1}{2} \mu_{ij|k} \mu^{ij|k} + \left(\mathcal{K} - \frac{\ddot{a}}{2a} \right) \mu_{ij} \mu^{ij} \right] \right\} \psi(\mu_{ij}, \eta). \quad (11)$$

This is the most simple form of the Schrödinger equation which governs tensor perturbations for a quantum minispace model with fluid matter source.

The equation for the modes $\mu_k = \omega_k/a$ which can be derived from Eq. (11) reads (for that point on, the k -index will be omitted)

$$\mu'' + \left(k^2 + 2\mathcal{K} - \frac{a''}{a} \right) \mu = 0, \quad (12)$$

which has the same form as the one obtained for classical backgrounds (see Ref. [1]), with the important difference that the function $a(\eta)$ is no longer the classical solution for the scale factor, but the quantum Bohmian solution. In this way, we can proceed with the usual analysis, with the quantum Bohmian solution $a(\eta)$ coming from Eq. (7) acting as the new pump field.

III. THE BACKGROUND BOHMIAN TRAJECTORIES

In order to obtain the background quantum solutions, we choose the following factor ordering for the kinetic term of the background Schrödinger equation (from now on $T = t$):

$$\begin{aligned} i \frac{\partial \varphi}{\partial t} &= -\frac{1}{4} \left[a^{(3\omega-1)/2} \hat{P}_a a^{(3\omega-1)/2} \hat{P}_a \right] \varphi - \mathcal{K} a^{3\omega+1} \varphi \\ &= \frac{1}{4} \left\{ a^{(3\omega-1)/2} \frac{\partial}{\partial a} \left[a^{(3\omega-1)/2} \frac{\partial}{\partial a} \right] \right\} \varphi - \mathcal{K} a^{3\omega+1} \varphi, \end{aligned} \quad (13)$$

which is the factor ordering yielding a covariant Schrödinger equation under field redefinitions [20].

The quantum Bohmian trajectories are obtained from the solutions of Eq. (13). There are two distinct situations: whether the spacelike hypersurfaces are flat or not.

A. Flat spatial sections

With the factor ordering chosen in Eq. (13) with $\mathcal{K} = 0$, we can change variables to $\chi = \frac{2}{3}(1-\omega)^{-1} a^{3(1-\omega)/2}$,

obtaining the simple equation

$$i \frac{\partial \varphi}{\partial t} = \frac{1}{4} \frac{\partial^2 \varphi}{\partial \chi^2}. \quad (14)$$

Note that this is just the time reversed Schrödinger equation for a one dimensional free particle constrained to the positive axis. As a and χ are positive, solutions which have unitary evolution must satisfy the condition

$$\varphi^* \frac{\partial \varphi}{\partial \chi} - \varphi \frac{\partial \varphi^*}{\partial \chi} \Big|_{\chi=0} = 0 \quad (15)$$

(see Ref. [4] for details).

We will choose the initial normalized wave function

$$\varphi_0(\chi) = \left(\frac{8}{t_0 \pi} \right)^{1/4} \exp \left(-\frac{\chi^2}{t_0} \right), \quad (16)$$

where t_0 is an arbitrary constant which determines the width of the Gaussian and hence the probability amplitude of initial scale factors. The Gaussian φ_0 satisfies condition (15). It is a commonly used initial condition when the time gauge is fixed and one gets a Schrödinger equation of the type of Eq. (14) [2, 4, 18], and even when the time gauge is not fixed when constructing wave packets [3, 21].

Using the propagator procedure of Refs. [2, 4], we obtain the wave solution for all times in terms of a :

$$\varphi(a, t) = \left[\frac{8t_0}{\pi(t^2 + t_0^2)} \right]^{1/4} \exp \left[\frac{-4t_0 a^{3(1-\omega)}}{9(t^2 + t_0^2)(1-\omega)^2} \right] \exp \left\{ -i \left[\frac{4ta^{3(1-\omega)}}{9(t^2 + t_0^2)(1-\omega)^2} + \frac{1}{2} \arctan \left(\frac{t_0}{t} \right) - \frac{\pi}{4} \right] \right\}. \quad (17)$$

Due to the chosen factor ordering, the probability density $\rho(a, t)$ has a non trivial measure and it is given by $\rho(a, t) = a^{(1-3\omega)/2} |\varphi(a, t)|^2$. Its continuity equation coming from Eq. (13) reads

$$\frac{\partial \rho}{\partial t} - \frac{\partial}{\partial a} \left[\frac{a^{(3\omega-1)}}{2} \frac{\partial S}{\partial a} \rho \right] = 0, \quad (18)$$

which implies in the Bohm interpretation that

$$\dot{a} = -\frac{a^{(3\omega-1)}}{2} \frac{\partial S}{\partial a}, \quad (19)$$

in accordance with the classical relations $\dot{a} = \{a, H\} = -\frac{1}{2} a^{(3\omega-1)} P_a$ and $P_a = \partial S / \partial a$.

Inserting the phase of (17) into Eq. (19), we obtain the Bohmian quantum trajectory for the scale factor:

$$a(t) = a_0 \left[1 + \left(\frac{t}{t_0} \right)^2 \right]^{\frac{1}{3(1-\omega)}}. \quad (20)$$

Note that this solution has no singularities and tends to the classical solution when $t \rightarrow \pm\infty$. Remember that we are in the gauge $N = a^{3\omega}$, and t is related to conformal time through

$$N dt = a d\eta \implies d\eta = [a(t)]^{3\omega-1} dt. \quad (21)$$

The solution (20) can be obtained for other initial wave functions (see Ref. [4]).

B. Curved spatial sections

In this case, only for $\omega = \frac{1}{3}$ (radiation) are there analytic solutions available. Here, $t = \eta$, and there is no factor ordering ambiguity in the kinetic term. Equation (7) [or (13)] reduces to the time reversed Schrödinger equation for harmonic or anharmonic oscillators. Now the condition for unitary evolution reads

$$\varphi^* \frac{\partial \varphi}{\partial a} - \varphi \frac{\partial \varphi^*}{\partial a} \Big|_{a=0} = 0, \quad (22)$$

the probability density $\rho(a, t)$ is the trivial one, namely $\rho(a, t) = |\varphi(a, t)|^2$, satisfying the continuity equation

$$\frac{\partial \rho}{\partial t} - \frac{\partial}{\partial a} \left(\frac{1}{2} \frac{\partial S}{\partial a} \rho \right) = 0, \quad (23)$$

yielding the guidance relation

$$\dot{a} = -\frac{1}{2} \frac{\partial S}{\partial a}. \quad (24)$$

Given the same initial wave function as before, we obtain (see Ref. [2]),

$$\varphi(a, \eta) = \left\{ \frac{8\eta_0 \mathcal{K}}{\pi \left[\eta_0^2 \mathcal{K} \cos^2(\sqrt{\mathcal{K}}\eta) + \sin^2(\sqrt{\mathcal{K}}\eta) \right]} \right\}^{1/4} \exp \left[\frac{-\eta_0 a^2 \mathcal{K}}{\eta_0^2 \mathcal{K} \cos^2(\sqrt{\mathcal{K}}\eta) + \sin^2(\sqrt{\mathcal{K}}\eta)} \right] \times$$

$$\times \exp \left(-i \left\{ \frac{(1 - \mathcal{K}\eta_0^2) \sqrt{\mathcal{K}} a^2 \cos(\sqrt{\mathcal{K}}\eta) \sin(\sqrt{\mathcal{K}}\eta)}{\left[\eta_0^2 \mathcal{K} \cos^2(\sqrt{\mathcal{K}}\eta) + \sin^2(\sqrt{\mathcal{K}}\eta) \right]} + \frac{1}{2} \arctan \left[\frac{\eta_0 \sqrt{\mathcal{K}} \cos(\sqrt{\mathcal{K}}\eta)}{\sin(\sqrt{\mathcal{K}}\eta)} \right] - \frac{\pi}{4} \right\} \right) \quad (25)$$

(we change t_0 to η_0 when $\omega = \frac{1}{3}$).

The Bohmian quantum scale factor obtained through the substitution of the phase of Eq. (25) into Eq. (24) reads

$$a(\eta) = a_0 \left[1 + \frac{(1 - \mathcal{K}\eta_0^2) \sin^2(\sqrt{\mathcal{K}}\eta)}{\mathcal{K}\eta_0^2} \right]^{\frac{1}{2}} = a_0 \left[\cos^2(\sqrt{\mathcal{K}}\eta) + \frac{\sin^2(\sqrt{\mathcal{K}}\eta)}{\mathcal{K}\eta_0^2} \right]^{\frac{1}{2}} \quad (26)$$

For $\mathcal{K} = 0$ and radiation, we can obtain the wave solution and Bohmian trajectories either by taking the respective limits from Eqs. (17) and (20) or Eqs (25) and (26). The resulting Bohmian scale factor is

$$a = a_0 \sqrt{1 + \left(\frac{\eta}{\eta_0} \right)^2}. \quad (27)$$

Note that, for the curved space section solutions be realistic, there must have a long epoch after the bounce when the scale factor recover its classical evolution and the curvature is negligible, i.e. when the scale factor in Eq. (26) can be approximated in some large interval of η to $a(\eta) \propto \eta$ in order for the model to be compatible with standard nucleosynthesis and cosmological observations. This can be accomplished if $\eta_0 \ll 1$. It means that the initial wave function (16) must be a very centered Gaussian around zero. The flatness problem is then translated to the quantum cosmological language to the question: why an initial Gaussian wave function of the Universe is so centered around a null value for the scale factor?

IV. TENSORIAL MODES PROPAGATION

Having obtained in the previous sections the propagation equation for the full quantum tensorial modes,

namely Eq. (12), in the Bohmian picture with the scale factor assuming the form (20) or (26), it is our goal in this section to solve this equation in order to obtain the gravitational wave power spectrum as predicted by such models. The first two subsections deal with the flat spatial section case for $-\frac{1}{3} < \omega < 1$. The final one treat the curved spatial cases for $\omega = \frac{1}{3}$.

A. Power spectrum for flat spatial section

Our first task consists in going from the conformal time η to the more convenient time variable t stemming from the change (21). With a dot indicating a derivative with respect to t , the mode potential reads

$$\frac{a''}{a} = a^{2(1-3\omega)} \left[\frac{\ddot{a}}{a} + (1-3\omega) \left(\frac{\dot{a}}{a} \right)^2 \right], \quad (28)$$

and Eq. (12) transforms into

$$\ddot{v} + \left[\frac{k^2 + 2\mathcal{K}}{a^{2(1-3\omega)}} - \frac{3}{4} (1-3\omega)(1-\omega) \left(\frac{\dot{a}}{a} \right)^2 - \frac{3}{2} (1-\omega) \frac{\ddot{a}}{a} \right] v = 0, \quad (29)$$

in which we have defined $v \equiv a^{\frac{1}{2}(1-3\omega)} \mu$. Specializing to the flat $\mathcal{K} = 0$ case and setting

$$v \equiv \ell_{\text{Pl}} \sqrt{t_0} \bar{v} \quad , \quad x \equiv \frac{t}{t_0} \quad \text{and} \quad \tilde{k} \equiv \frac{k}{k_0} \quad \text{with} \quad \bar{k}_0 \equiv (t_0 a_0^{3\omega-1})^{-1},$$

we obtain

$$\frac{d^2 \bar{v}}{dx^2} + \left[\tilde{k}^2 (1+x^2)^{\frac{2(3\omega-1)}{3(1-\omega)}} - \frac{1}{(1+x^2)^2} \right] \bar{v} = 0. \quad (30)$$

which is in a useful form for the practical purpose of numerical resolution. We shall assume the usual vacuum

state initial condition for the modes, *i.e.* we set [1]

$$\mu_{\text{ini}} = \frac{\sqrt{3}\ell_{\text{Pl}}}{\sqrt{k}} \exp[-ik(\eta - \eta_{\text{ini}})], \quad (31)$$

where η_{ini} is an arbitrary (and physically irrelevant as was checked numerically) constant conformal time, which we set to zero in what follows without loss of generality. Figs. 1 to 3 show the actual mode calculated numerically with Eq. (30).

The power spectrum can now be defined as [1]

$$k^3 \mathcal{P}_h \equiv \frac{2k^3}{\pi^2} \left| \frac{\mu}{a} \right|^2, \quad (32)$$

leading to

$$k^3 \mathcal{P}_h = \frac{2\tilde{k}^3}{\pi^2} \tilde{k}_0^2 \frac{|\bar{v}|^2}{1+x^2} \left(\frac{\ell_{\text{Pl}}}{a_0} \right)^2, \quad (33)$$

which, although in general being a time-dependent quantity, happens to be constant in the expanding phase for the time period we are interested in. Therefore, it suffices to solve Eq. (30) with the initial condition (31) to obtain the gravitational wave power spectrum we are seeking. This is how we obtained the figures.

B. Piecewise approximation and matching in the flat spatial section case

1. Asymptotic behaviors

Given Eq. (20) and the relation (21) between the two time parameters, one has

$$\eta = a_0^{1-3\omega} {}_2\mathcal{F}_1 \left[\frac{1}{2}, \frac{3\omega-1}{3(\omega-1)}, \frac{3}{2}, -\left(\frac{t}{t_0}\right)^2 \right] t, \quad (34)$$

where ${}_2\mathcal{F}_1$ is a hypergeometric function and we have assumed a common origin for both times (*i.e.* $\eta = 0$ for $t = 0$). This can be simplified by considering that one is mostly interested, either for setting initial conditions or for observing the resulting power spectrum, for times much larger than the typical bounce duration, *i.e.* for $t \gg t_0$. Then, one recovers the usual perfect fluid power law solution for the scale factor, allowing us to write

$$k\eta = \pm \frac{3(1-\omega)}{1+3\omega} \tilde{k}|x|^{\frac{1+3\omega}{3(1-\omega)}}, \quad (35)$$

where the sign is to be determined by that of x .

Eq. (12) with $\mathcal{K} = 0$ has a potential for gravitational waves that is written $V_{\text{grav}} = a''/a$, and which can be expressed in terms of the x variable as

$$V_{\text{grav}} = A (1+x^2)^{\frac{4}{3(\omega-1)}} [(3\omega-1)x^2 + 3(\omega-1)], \quad (36)$$

where the constant A is given by

$$A = -\frac{2}{9} \left[\frac{a_0^{1-3\omega}}{(\omega-1)t_0} \right]^2.$$

For large values of η , hence of x , and provided $\omega \neq \frac{1}{3}$, one gets

$$V_{\text{grav}} \sim (3\omega-1)Ax^{\frac{2(3\omega+1)}{3(\omega-1)}}, \quad (37)$$

which vanishes asymptotically for all cases of practical interest ($-1/3 \leq \omega \leq 1$).

The case $\omega = 1/3$ is a very special and simple one: the time t is conformal time η , Eq. (29 is identical to Eq. (12), and $a(\eta) = a_0[1 + (\eta/\eta_0)^2]^{1/2}$. In a different context, this same mode equation (with $\mathcal{K} = 0$) was treated in Ref. [22], yielding an spectral index $k^3 \mathcal{P}_h \propto k^{n_{\text{T}}}$ given by $n_{\text{T}} = 2$.

2. Matching points

Let us determine the end of potential domination point, denoted by x_{M} in what follows, *i.e.*, the time at which $k^2 = a''(x_{\text{M}})/a(x_{\text{M}})$. This is

$$x_{\text{M}} = \left[\frac{9(1-\omega)^2}{2|1-3\omega|} \tilde{k}^2 \right]^{\frac{3(\omega-1)}{2(1+3\omega)}}. \quad (38)$$

This point will also be used to match different solutions and thus propagate the mode through the bounce.

It is interesting to note that the corresponding point for the evolution of \bar{v} , namely the point obtained by annihilating the bracket in Eq. (30), called x_{exit} , is

$$x_{\text{exit}} = \sqrt{\tilde{k}^{\frac{3}{2}(\omega-1)} - 1} \simeq \tilde{k}^{\frac{3}{4}(\omega-1)},$$

so that the ratio is

$$\frac{x_{\text{exit}}}{x_{\text{M}}} \propto \tilde{k}^{\frac{9}{4} \frac{(1-\omega)^2}{1+3\omega}} \ll 1, \quad (39)$$

which, for long wavelengths ($\tilde{k} \ll 1$) is much less than one (recall that $-1/3 < \omega < 1$). Therefore, the modes we consider in the numerical solution have no time to start oscillating before reaching x_{M} .

3. Solutions

Putting Eq. (37) into Eq. (12) and using (35), we arrive at the conclusion that, sufficiently far from the bounce, the perturbation mode satisfies

$$\mu'' + \left[k^2 + \frac{2(3\omega-1)}{(1+3\omega)^2 \eta^2} \right] \mu = 0, \quad (40)$$

whose solution is

$$\mu = \sqrt{\eta} \left[c_1(k) H_{\nu}^{(1)}(k\eta) + c_2(k) H_{\nu}^{(2)}(k\eta) \right], \quad (41)$$

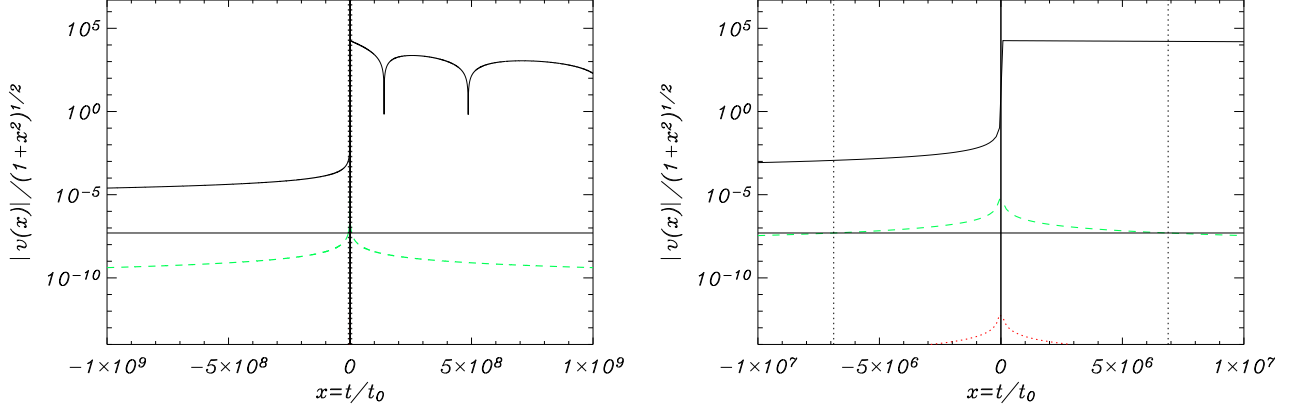


FIG. 1: Time evolution of the mode function \bar{v} for the equation of state $\omega = 0.1$ and wavenumber $\tilde{k}^2 = 5 \times 10^{-8}$. The full line is $|\bar{v}(x)|/\sqrt{1+x^2} = \mu/a$ and thus provides directly the power spectrum. The symmetric curves are background functions: dashed is the conformal time potential a''/a as given by Eq. (28), dotted is the term proportional to \tilde{k}^2 in Eq. (29) and full is $(1+x^2)^{-2}$. The horizontal thin straight line gives the value of \tilde{k}^2 used to compute the figures. The left panel shows the full time evolution which was computed. For $x < 0$, there are oscillations only in the real and imaginary parts of the mode, so the amplitude shown is a non oscillating function of time. It however acquires an oscillating piece after the bounce has taken place. The right panel is merely a zoom for smaller time scales also showing $\pm x_M$ (the dotted vertical line) and x_{exit} (the full vertical line, indistinguishable on that scale with the axis). One clearly sees that even though the mode indeed starts oscillating, it does so on a timescale such that it is approximately constant all the way to x_M .

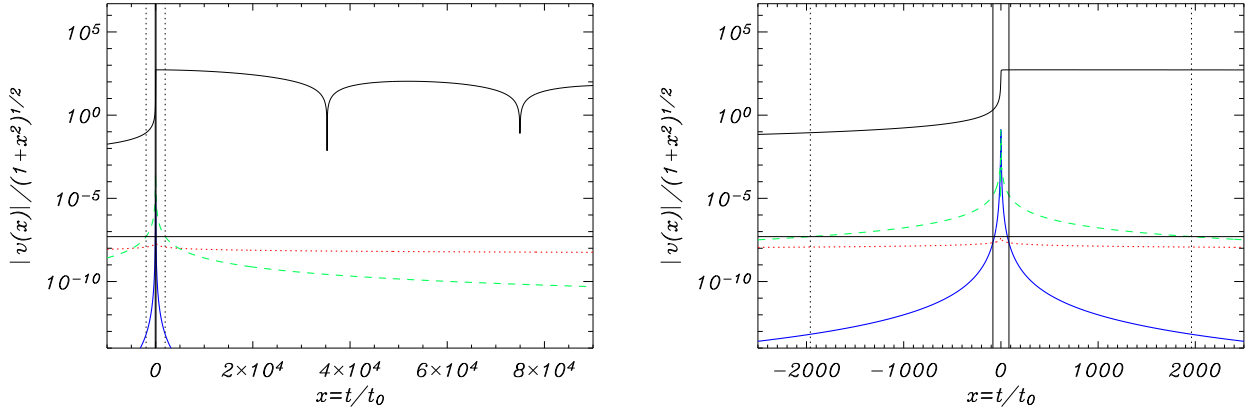


FIG. 2: Same as Fig. 1 with $\omega = 0.3$. The oscillations are visible on the left panel and the detailed view of the right panel emphasizes that there is no discontinuity on the mode. It also shows both matching points.

with

$$\nu = \frac{3(1-\omega)}{2(3\omega+1)},$$

c_1 and c_2 being two constants depending on the wavelength, $H^{(1,2)}$ being Hankel functions.

This solution applies asymptotically, where one can impose initial conditions on the mode, as well as in the matching region for which $V_{\text{grav}} \sim k^2$, provided $\tilde{k}^2 \ll 1$. Demanding the Bunch-Davies vacuum normal-

ization (31) then implies

$$c_1 = 0 \quad \text{and} \quad c_2 = \ell_{\text{Pl}} \sqrt{\frac{3\pi}{2}} e^{-i\frac{\pi}{2}(\nu+\frac{1}{2})}.$$

The solution can also be expanded in powers of k^2 according to the formal solution [1]

$$\begin{aligned} \frac{\mu}{a} - \mathcal{O}(k^{j \geq 4}) &= A_1(k) \left[1 - k^2 \int^t \frac{d\bar{\eta}}{a^2(\bar{\eta})} \int^{\bar{\eta}} a^2(\bar{\eta}) d\bar{\eta} \right] \\ &+ A_2(k) \left[\int^\eta \frac{d\bar{\eta}}{a^2} - k^2 \int^\eta \frac{d\bar{\eta}}{a^2} \int^{\bar{\eta}} a^2 d\bar{\eta} \int^{\bar{\eta}} \frac{d\bar{\eta}}{a^2} \right], \end{aligned} \quad (42)$$

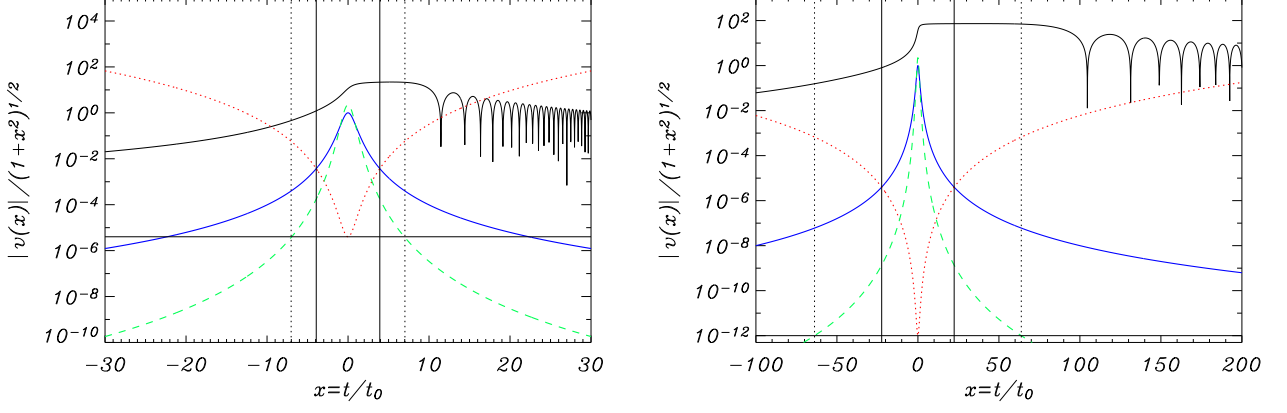


FIG. 3: Same as previous figures with $\omega = 0.7$ and two different wavenumbers $\tilde{k} = 2 \times 10^{-3}$ (left) and $\tilde{k} = 10^{-6}$ (right).

where A_1 and A_2 are two constants depending only on the wavenumber k through the initial conditions. Neglecting the $\mathcal{O}(k^2)$ terms, for the expanding phase, the A_2 term is known as the decaying mode, and the power spectrum (32) can then be approximated accurately by a constant; this constant power spectrum is the one we are looking for. Although this form is particularly valid as long as $k^2 \ll a''/a$, i.e. when the mode is below its potential, Eq. (42) should formally apply for all times. In the matching region, the $\mathcal{O}(k^2)$ terms may give contributions to the amplitude, but they do not alter the k -dependence of the power spectrum.

For the solution (20), the leading order of the solution (42) reads

$$\begin{aligned} \frac{\mu}{a} &= A_1 + A_2 t_0 a_0^{3(\omega-1)} \arctan x \\ &\sim A_1 - A_2 t_0 a_0^{3(\omega-1)} \left(\frac{\pi}{2} + \frac{1}{x} \right), \\ \implies \mu &\sim \tilde{A}_1 x^{\frac{2}{3(1-\omega)}} + \tilde{A}_2 x^{\frac{3\omega-1}{3(1-\omega)}}, \end{aligned} \quad (43)$$

where in the last steps we have taken the limit $x \rightarrow -\infty$ and identified the leading orders in x , with $\tilde{A}_1 = A_1 a_0 - \frac{\pi}{2} a_0^{3\omega-2} t_0 A_2$ and $\tilde{A}_2 = -a_0^{3\omega-2} t_0 A_2$. Propagating this solution on the other side of the bounce, in the expanding epoch, yields the required power spectrum, i.e. the limit for $x \rightarrow +\infty$, namely

$$\left. \frac{\mu}{a} \right|_{\text{const}} \sim A_1 + \frac{\pi}{2} a_0^{3(\omega-1)} t_0 A_2 = \frac{1}{a_0} (\tilde{A}_1 - \pi \tilde{A}_2), \quad (44)$$

where we have taken only the constant part of the modes.

4. Matching and spectrum

In order to get the spectrum of gravitational waves produced by our bouncing model, it suffices to match μ and μ' at η_M , corresponding to x_M given by (38) through (35).

At this point, the mode function (41) and its derivative read

$$\mu(\eta_M) = \frac{C}{\sqrt{k}} \quad \text{and} \quad \mu'(\eta_M) = D\sqrt{k}, \quad (45)$$

where the constants C and D are given by

$$C = c_2 \sqrt{k\eta_M} H_\nu^{(2)}(k\eta_M), \quad (46)$$

and

$$\begin{aligned} D &= \frac{c_2}{2} \left\{ \frac{H_\nu^{(2)}(k\eta_M)}{\sqrt{k\eta_M}} \right. \\ &\quad \left. + \sqrt{k\eta_M} [H_{\nu-1}^{(2)}(k\eta_M) - H_{\nu+1}^{(2)}(k\eta_M)] \right\}, \end{aligned} \quad (47)$$

with

$$k\eta_M = \frac{\sqrt{2|1-3\omega|}}{1+3\omega}.$$

This is also expressed as

$$\mu(\eta_M) = \frac{\tilde{C}}{\sqrt{k}} \quad \text{and} \quad \mu'(\eta_M) = \tilde{D}\sqrt{k}, \quad (48)$$

with $\tilde{C} = \sqrt{t_0} a_0^{(3\omega-1)/2} C$ and $\tilde{D} = a_0^{(1-3\omega)/2} D / \sqrt{t_0}$.

Matching μ [Eqs. (43) and (45)] and its derivative with respect to conformal time, namely $\mu' = a^{1-3\omega} t_0^{-1} d\mu/dx$, one obtains, to leading order

$$\tilde{A}_1 = \left[\frac{3\omega-1}{3\alpha(\omega-1)} \tilde{C} + a_0^{3\omega-1} t_0 \beta \tilde{D} \right] \tilde{k}^{\frac{3(1-\omega)}{2(3\omega+1)}}, \quad (49)$$

$$\tilde{A}_2 = \left[\frac{2}{3\beta(1-\omega)} \tilde{C} - a_0^{3\omega-1} t_0 \alpha \tilde{D} \right] \tilde{k}^{\frac{3(\omega-1)}{2(3\omega+1)}}, \quad (50)$$

with

$$\alpha = \left[\frac{9(1-\omega)^2}{2|1-3\omega|} \right]^{-1/(1+3\omega)}$$

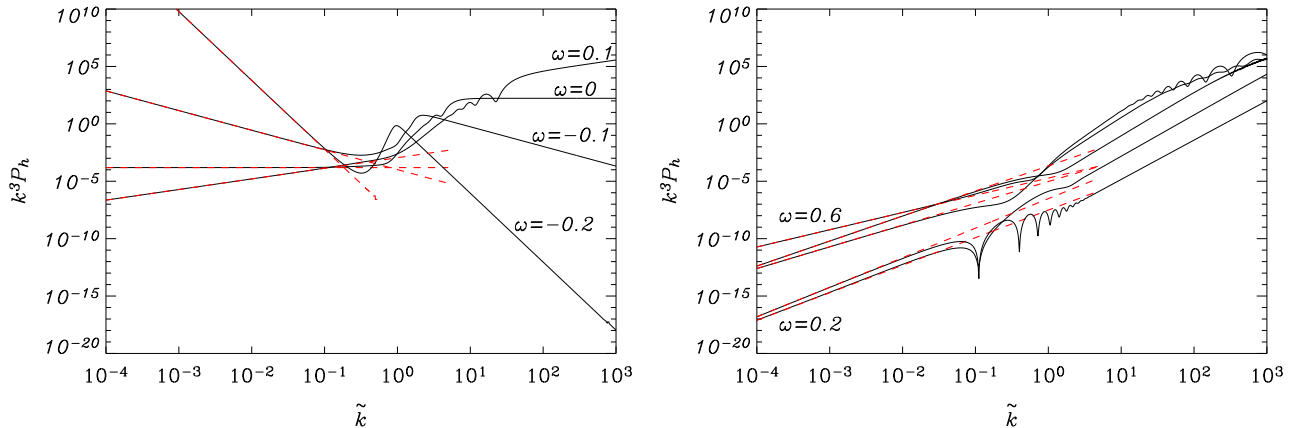


FIG. 4: Power spectra for different values of the state parameter ω . The dashed lines represent the approximation (51) with the power index given by Eq. (52), while the full lines are the spectra obtained by numerically solving Eq. (30). Shown on the right panel are solutions for $\omega \in \{0.2, 0.3, 0.4, 0.5, 0.6\}$.

and

$$\beta = \left[\frac{9(1-\omega)^2}{2|1-3\omega|} \right]^{\frac{1-3\omega}{2(1+3\omega)}}.$$

The coefficients \tilde{A}_1 and \tilde{A}_2 contain each a power-law behaviors in k . Because $\omega < 1$, the power in \tilde{A}_2 [Eq. (50)] is negative definite and that in \tilde{A}_1 [Eq. (49)] is positive definite. Therefore, \tilde{A}_2 is the dominant mode and gives the spectral index, while \tilde{A}_1 provides the sub-dominant mode that happens, incidentally, to correspond to an unaltered propagation of the initial conditions. One then gets the spectrum (44), and finally the spectral index n_{τ} writing

$$k^3 \mathcal{P}_h \propto k^{n_{\tau}}, \quad (51)$$

and we get

$$n_{\tau} = \frac{12\omega}{1+3\omega} \quad (52)$$

Note that the limit $\omega \rightarrow \frac{1}{3}$ of Eq. (52) gives the correct index for radiation (see Ref. [22]), although the calculation, in this case, should not be valid; this is due to the expected continuity of the spectral index with the equation of state. The spectrum as calculated numerically is plotted on Fig 4 for various values of ω together with the approximation (52).

It is interesting to note that this result was also presented in the semiclassical approximation (classical background and quantum perturbations) in Ref. [23]. In Ref. [23], the asymptotic behaviors both in the past and future infinities are two, possibly different, power laws for the contraction and expansion phases, whereas the type of bounces we studied here is restricted to equal asymptotic behaviors, i.e., for $|t| \gg t_0$. Since the potentials in the equations for μ are smooth and large compared to

k around the bounce, it looks like the full quantum effects and details of the bounce do not change significantly the main spectral features of the gravitational wave produced. It would be interesting to verify if this results still holds for other bounces, e.g. those having different asymptotic behaviors and/or more complicated shapes of the potential for μ . In this last situation, and if the results of Ref. [12] apply, one would expect the actual spectra to be different.

C. Power spectrum for curved spatial sections and radiation

In this subsection we consider the power spectrum of tensor perturbations for quantum cosmological backgrounds with curved spatial sections. As mentioned in Sec. III, only in the radiation case one can obtain analytic solutions for the quantum background. Hence, we will restrict ourselves to this fluid from now on.

Inserting Eq. (26) into Eq. (12), and noting that $k^2 = m^2 - 3\mathcal{K}$, where m is an integer greater or equal to 3 for $\mathcal{K} = 1$, and a real number greater than zero for $\mathcal{K} = -1$, we obtain

$$\mu'' + \left\{ m^2 - \frac{\eta_0^2}{[\eta_0^2 \mathcal{K} \cos^2(\sqrt{\mathcal{K}}\eta) + \sin^2(\sqrt{\mathcal{K}}\eta)]^2} \right\} \mu = 0. \quad (53)$$

The effective potential

$$V_{\text{eff}} = \frac{\eta_0^2}{[\eta_0^2 \mathcal{K} \cos^2(\sqrt{\mathcal{K}}\eta) + \sin^2(\sqrt{\mathcal{K}}\eta)]^2} \quad (54)$$

has one maximum given by $1/\eta_0^2$ and goes to zero when $\eta \rightarrow \infty$ for $\mathcal{K} = -1$. It oscillates between $1/\eta_0^2$ and η_0^2 , which are respectively a maximum and a minimum provided $\eta_0 < 1$, when $\mathcal{K} = +1$. Indeed, as we have seen in

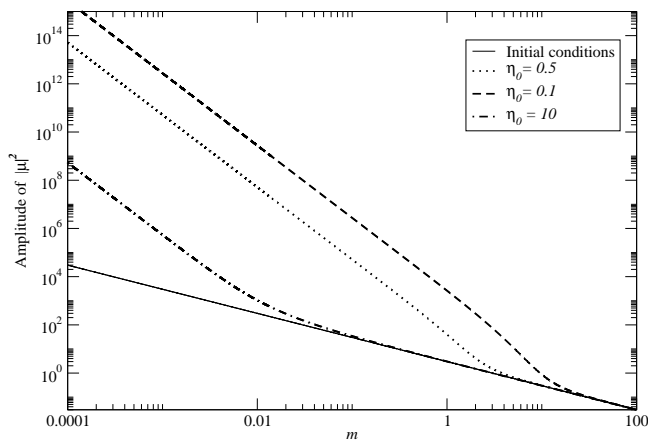


FIG. 5: Amplitude amplification of the gravitational modes in the $\mathcal{K} = -1$ curved case filled with radiation. For $m \ll 1$, the amplitude behaves, as expected at least for the case $\eta_0 \ll 1$, as a power law since then $\mu \propto m^{-3/2} \sin m\eta$.

Sec. III, in order for the background models to be realistic, one must have $\eta_0 \ll 1$. Hence, the maxima of the effective potential are very high in both cases and the minima are very small in the $\mathcal{K} = 1$ case. Large wavelengths (small m) will cross the effective potential and the perturbations will be amplified at each bounce. This induces an instability of the model because this enhancement happens an infinite number of times, and therefore, however small the initial perturbation might have been, there is a time at which the linear theory is no longer valid and the cosmological setup breaks down.

For $\mathcal{K} = -1$, the situation is very similar to the flat case. The conformal time (η_M) of potential crossing is given as the solution of the equation

$$\sinh(\eta_M) = \pm \sqrt{\left(\frac{1}{m\eta_0} - 1\right) \frac{\eta_0}{\sqrt{1 + \eta_0^2}}}, \quad (55)$$

which has a real solution provided $m\eta_0 < 1$. Thus, the mode crosses the potential only in this case. This constraint is however satisfied for the situations we are interested in, namely, $\eta_0 \ll 1$ and $m \ll 1$. One then obtains

$$|\eta_M| \approx \operatorname{arcsinh}\left(\sqrt{\frac{\eta_0}{m}}\right). \quad (56)$$

We have two limiting cases, namely $\eta_0 \gg m$ and $\eta_0 \ll m$ yielding, respectively,

$$|\eta_M| \approx \ln[2(\eta_0/m)^{1/2}], \quad (57)$$

and

$$|\eta_M| \approx (\eta_0/m)^{1/2}. \quad (58)$$

The effect of the potential for μ is to increase its amplitude by a factor shown on Fig. 5, as well as to mix the exponential terms. This can be easily seen by the

following approximation. For $\eta_0 \ll 1$, the maximum of the effective potential at $\eta = 0$ is very large while for $\eta \gg \eta_0$ it behaves like $\eta_0^2/\sinh^4(\eta)$, which goes to zero when $\eta_0 \rightarrow 0$. Hence the effective potential (54) can be well approximated to a Dirac delta in this limit. Its integration reads

$$\begin{aligned} \int V_{\text{eff}}(\eta) d\eta &= \frac{1}{\eta_0^2} \int d\eta \left[1 + \left(1 + \frac{1}{\eta_0^2} \right) \sinh^2 \eta \right]^{-2} \\ &= \frac{(\eta_0^2 + 1) \sinh(2\eta)}{2[(\eta_0^2 - 1) + (\eta_0^2 + 1) \cosh(2\eta)]} \\ &\quad + \frac{1 - \eta_0^2}{2\eta_0} \tan^{-1} \left(\frac{\tanh \eta}{\eta_0} \right), \end{aligned} \quad (59)$$

which implies

$$\int_{-\infty}^{\infty} V_{\text{eff}}(\eta) d\eta = 1 + \frac{1 - \eta_0^2}{\eta_0} \tan^{-1} \frac{1}{\eta_0} \simeq \frac{\pi}{2\eta_0} + \mathcal{O}(\eta_0), \quad (60)$$

where in the last step we have assumed that $\eta_0 \ll 1$.

Hence, one can approximate the effective potential by a Dirac distribution [12] $\pi\delta(\eta)/2\eta_0$. The solution for $\eta \neq 0$ is then simply Eq. (31) with k substituted by m for $\eta < 0$, and $\mu = Ae^{im\eta} + Be^{-im\eta}$ for $\eta > 0$. Demanding that μ be continuous across the potential and imposing Eq. (53) then leads to another matching condition, namely

$$\mu'(0^+) - \mu'(0^-) = \frac{\pi}{2\eta_0} \mu(0). \quad (61)$$

One then finds that

$$\begin{aligned} A &= -\frac{i\pi\sqrt{3}\ell_{\text{Pl}}}{4\eta_0 m^{3/2}}, \\ B &= \frac{i\pi\sqrt{3}\ell_{\text{Pl}}}{4\eta_0 m^{3/2}} + \sqrt{\frac{3}{m}} \ell_{\text{Pl}}, \end{aligned} \quad (62)$$

and finally, in the long wavelength approximation for which $m \ll 1$, that $\mu \propto m^{-3/2} \sin m\eta$. This is exactly what is obtained numerically, as shown on Fig. 5. Note also that when the curves reach the $m\eta_0 > 1$ region, the amplitude is the initial one: the mode has not crossed the potential as explained above.

Note incidentally that solution (62) is exactly the same as the one obtained in Ref. [22] and in the present paper for radiation with $\mathcal{K} = 0$, where we used the matching method. This is because also in this case one can approximate the potential to a Dirac distribution as $V \approx \eta_0^2/\eta^4$ when $\eta \gg \eta_0$, which goes to zero in the limit $\eta_0 \rightarrow 0$. However, for the parabolic scale factor $a(\eta) = a_0[1 + (\eta/\eta_0)^2]$ also treated in Ref. [22], which solutions are quite different from (62), the potential is $V = 1/(\eta^2 + \eta_0^2)$, whose limit for $\eta \gg \eta_0$ is $1/\eta^2$, independent of η_0 . Hence in this case, the effective potential cannot be approximated by a Dirac distribution, and the final spectrum is very different. We thus confirm that the power spectrum of perturbations through a bounce may depend significantly of the details of the bounce itself.

With the coefficients (62), one can calculate the spectrum

$$m^3 \mathcal{P}_h \equiv \frac{2m^3}{\pi^2} \left| \frac{\mu}{a} \right|^2, \quad (63)$$

for the two possible matching points (57,58), yielding $m^3 \mathcal{P}_h \propto m^3 \ln^2(m)$ and $m^3 \mathcal{P}_h = m^2$. Note that, as expected, the case $\eta_0 \ll m$ yields the same spectrum as the flat case: the two scale factors are quite similar in that limit.

V. CONCLUSION

We have obtained the power spectrum of tensor perturbations in bouncing quantum cosmological models with a perfect fluid satisfying $p = \omega\rho$ for flat spatial sections and $-\frac{1}{3} < \omega < 1$, and for curved spatial sections with $\omega = \frac{1}{3}$. For flat spatial sections, the spectral index for large wavelengths is $n_T = 12\omega/(1+3\omega)$. The positive curved spatial section model is unstable, while the negative curved spatial section model amplifies the modes, changing the amplitude to a power index of $n_T \approx 3$ or $n_T = 2$, depending on the parameters. All cases lead to oscillations in the primordial spectrum.

The most interesting case is the one of radiation, which is the best perfect fluid model for the early Universe (all particles are ultra-relativistic). For almost flat spatial sections we have $n_T \approx 2$, which is different from the predictions of inflation. Hence, this model can be po-

tentially tested against inflation in future observations, specially concerning the polarization of the cosmic microwave background, Planck observations, and gravitational wave detectors if we calculate the amplitude of these perturbations.

The next step would be to calculate the spectrum of scalar perturbations of these models. The dynamical equations for scalar perturbations are not, however, as simple as Eq. (12). The steps we have taken in Sec. (2) in order to arrive at Eq. (12) in the case where the background is also quantized are not so simple in the case of scalar perturbations, specially due to the matter terms. This is work in progress. Attainment of the power spectrum of scalar perturbations is crucial not only to test the model against WMAP observations, but also to calibrate and obtain the precise spectrum of tensor perturbations for possible comparisons with LIGO and VIRGO future data.

VI. ACKNOWLEDGMENTS

We would like to thank CNPq of Brazil for financial support. We would also like to thank both the Institut d'Astrophysique de Paris and the Centro Brasileiro de Pesquisas Físicas, where this work was done, for warm hospitality. We very gratefully acknowledge various enlightening conversations with Jérôme Martin. We also would like to thank CAPES (Brazil) and COFECUB (France) for partial financial support.

-
- [1] V. F. Mukhanov, H. A. Feldman, and R. H. Brandenberger, *Phys. Rep.* **215**, 203 (1992).
- [2] J. Acacio de Barros, N. Pinto-Neto, and M. A. Sagiore-Leal, *Phys. Lett. A* **241**, 229 (1998).
- [3] R. Colistete Jr., J. C. Fabris, and N. Pinto-Neto, *Phys. Rev. D* **62**, 083507 (2000).
- [4] F.G. Alvarenga, J.C. Fabris, N.A. Lemos and G.A. Monerat, *Gen.Rel.Grav.* **34**, 651 (2002).
- [5] See e.g. P. Holland, *The Quantum Theory of Motion*, Cambridge University Press (Cambridge, UK, 1993) and references therein.
- [6] N. Pinto-Neto and E. Sergio Santini, *Phys. Rev. D* **59**, 123517 (1999).
- [7] P. Peter, E. Pinho, and N. Pinto-Neto, *JCAP* **07**, 014 (2005).
- [8] A. Guth, *Phys. Rev. D* **23**, 347 (1981); A. Linde, *Phys. Lett. B* **108**, 389 (1982); A. Albrecht and P. J. Steinhardt, *Phys. Rev. Lett.* **48**, 1220 (1982); A. Linde, *Phys. Lett. B* **129**, 177 (1983); A. A. Starobinsky, *Pis'ma Zh. Eksp. Teor. Fiz.* **30**, 719 (1979) [*JETP Lett.* **30**, 682 (1979)]; V. Mukhanov and G. Chibisov, *JETP Lett.* **33**, 532 (1981); S. Hawking, *Phys. Lett. B* **115**, 295 (1982); A. A. Starobinsky, *Phys. Lett. B* **117**, 175 (1982); J. M. Bardeen, P. J. Steinhardt, and M. S. Turner, *Phys. Rev. D* **28**, 679 (1983); A. Guth, S. Y. Pi, *Phys. Rev. Lett.* **49**, 1110 (1982).
- [9] G. Veneziano, *Phys. Lett. B* **265**, 287 (1991); M. Gasperini and G. Veneziano, *Astropart. Phys.* **1**, 317 (1993); See also J. E. Lidsey, D. Wands, and E. J. Copeland, *Phys. Rep.* **337**, 343 (2000) and G. Veneziano, in *The primordial Universe*, Les Houches, session LXXI, edited by P. Binétruy *et al.*, (EDP Science & Springer, Paris, 2000)
- [10] J. Khoury, B. A. Ovrut, P. J. Steinhardt, and N. Turok, *Phys. Rev. D* **64**, 123522 (2001); [hep-th/0105212](#); R. Y. Donagi, J. Khoury, B. A. Ovrut, P. J. Steinhardt, and N. Turok, *JHEP* **0111**, 041 (2001).
- [11] G. Murphy, *Phys. Rev.* **D8**, 4231 (1973); A. A. Starobinsky, *Sov. Astron. Lett.* **4**, **82** (1978); M. Novello and J. M. Salim, *Phys. Rev.* **D20**, 377 (1979); V. Melnikov and S. Orlov, *Phys. Lett* **A70**, 263 (1979); P. Peter and N. Pinto-Neto, *Phys. Rev. D* **65**, 023513 (2002); P. Peter and N. Pinto-Neto, *Phys. Rev. D* **66**, 063509 (2002); V.A. De Lorenci, R. Klippert, M. Novello and J.M. Salim, *Phys. Rev. D* **65**, 063501 (2002); J. C. Fabris, R. G. Furtado, P. Peter and N. Pinto-Neto *Phys. Rev. D* **67**, 124003 (2003); P. Peter, N. Pinto-Neto and D. A. Gonzalez, *JCAP* **0312**, 003 (2003).
- [12] J. Martin and P. Peter, *Phys. Rev. Lett.* **92**, 061301 (2004).
- [13] A. Borde and A. Vilenkin, *Phys. Rev. D* **56**, 717 (1997).
- [14] J. Martin and R. Brandenberger, *Phys. Rev. D* **63**,

- 123501 (2001); R. Brandenberger and J. Martin, Mod. Phys. Lett. A **16**, 999 (2001); J. Niemeyer, Phys. Rev. D **63**, 123502 (2001); A. A. Starobinsky, JETP Lett. **73**, 371 (2001); M. Lemoine, M. Lubo, J. Martin, and J. P. Uzan, Phys. Rev. D **65**, 023510 (2002).
- [15] D. N. Spergel *et al.*, Ap. J. Suppl. **148**, 175 (2003); D. N. Spergel *et al.*, [astro-ph/0603449](#), Ap. J. (2006).
- [16] J. J. Halliwell and S. W. Hawking, Phys. Rev. D **31**, 1777 (1985).
- [17] B. F. Schutz, Jr., Phys. Rev. D **2** 2762 (1970); Phys. Rev. D **4**, 3559 (1971).
- [18] V. G. Lapchinskii and V. A. Rubakov, Theor. Math. Phys. **33**, 1076 (1977); F. Tipler, Phys. Rep. **137**, 231 (1986); N. Lemos, J. Math. Phys. **37** 1449 (1996).
- [19] K. V. Kuchar and C. G. Torre, Phys. Rev. **D43**, 419 (1991).
- [20] S. W. Hawking and D. N. Page, Nucl. Phys. **B264**, 185 (1986); T. Christodoulakis and J. Zanelli, Class. Quantum Grav. **4** (1987).
- [21] M. P. Dabrowski and C. Kiefer, Phys.Lett. **B397**, 185 (1997).
- [22] J. Martin, P. Peter, N. Pinto-Neto, and D. J. Schwarz, Phys. Rev. D **65**, 123513 (2002).
- [23] A. A. Starobinsky, JETP Lett. **30**, 682 (1979).